Rahul et al. 2018. *Int. J. Vehicle Structures & Systems*, 10(5), 337-341
ISSN: 0975-3060 (Print), 0975-3540 (Online)
doi: 10.4273/ijvss.10.5.06
© 2018. MechAero Foundation for Technical Research & Education Excellence

International Journal of Vehicle Structures & Systems
Available online at www.maftree.org/eja

Experimental Investigation and Optimization of SiC Abrasive Water Jet Machining of Aluminium Alloys

R. Rahul[a], S. Sreenivash[b], K. Renuka[c], S. Sathish[d] and V. Ananda Krishnan[e]

Dept. of Production Engg., National Institute of Tech., Tiruchirapalli, Tamil Nadu, India
[a]Corresponding Author, Email: rahulramaswamy97@gmail.com
[b]Email: sreenivash774@gmail.com
[c]Email: renukakhatravath@gmail.com
[d]Email: sadish.kss@nitt.edu
[e]Email: krishna@nitt.edu

ABSTRACT:

Investigation of the parameters variation over the abrasive water jet machining of aluminium 2014 alloy was studied using the Taguchi technique. Traverse speed, standoff distance, pressure and mass flow rate were considered as the process parameters and were varied at three levels. The depth of cut was taken as the response, and it was measured and analysed statistically. The optimal parameters to achieve the maximum depth of cut were identified with the main effect plot. Most influencing parameters over the depth of cut were identified with the analysis of variance and response table. A mathematical relationship was developed to predict the depth of cut.

KEYWORDS:

Water jet machining; Aluminium alloy; Taguchi methodology; Depth of cut; Optimization

CITATION:

R. Rahul, S. Srinivash, K. Renuka, S. Sathish and V.A. Krishnan. 2018. Experimental Investigation and Optimization of SiC Abrasive Water Jet Machining of Aluminium Alloys, *Int. J. Vehicle Structures & Systems*, 10(5), 337-341. doi:10.4273/ijvss.10.5.06.

1. Introduction

Abrasive water jet (AWJ) machining, a dominant process which solves the machining requirements of automobile and aerospace industry, due to its ability to machine wide variety of materials with higher material removal rates, complex contours and without heat affected zones. AWJ machining has led many researchers in their own niche to experiment with various materials and capabilities of the process. Aluminium alloy (AA) 2014 is of great industrial importance, especially as a structural member in large quantities and fuel tank housings. As early as 1994, Hocheng et al [1] studied the effect of various parameters such as the hydraulic pressure, abrasive flow rate and traverse speed on the material removal in cutting of ceramic plates by AWJ process and identified a certain threshold combination of parameters below which there is no material removal.

Choi et al [2] conducted experiments on Alumina ceramics and developed an analytical model and further explained the mechanism behind the brittle fracture during the machining. Momber and Kovacevic [3] studied the influence of process parameters during AWJ cutting of artificial rocklike materials, using linear regression analysis and identified a certain threshold combination of parameters for minimal material removal. The very first attempt at studying the application of AWJ process in the milling of fibre-reinforced plastics was tested by Hocheng et al [4] and formulated a relation between material removal rate and its input parameters. Wang et al [5] designed a statistical experiment to study the effect of process parameters on cutting of hot-dipped aluminium/zinc alloy coated structural steel sheet and identified an optimum parameter with a regression model. Huang et al [6] studied the effect of process parameters on high pressure AWJ cutting on granite and the identified the individual effects of each parameter comprehensively.

Azmir et al [7] designed a Taguchi-method based experiment to study the effect of various process parameters on the AWJ machining of Aramid fiber reinforced plastics and identified the most predominant parameter by analysis of variance. Axinte et al [8] investigated the application of AWJ cutting to cut polycrystalline diamond, a material known to possess extreme levels of hardness and thereby the investigation recorded the parameter combination to provide a through cut for a given length of material. Kechagias et al [9] conducted six set of experiments on TRIP sheet steels, in order to analyse the surface roughness and mean kerf generated in AWJ machining. In a similar approach, Gupta et al [10] used the ANOVA analysis and minimized the kerf taper and kerf width on the AWJ machining of marble. Kartal et al [11] optimized the parameters for machining of low density polyethylene by AWJ machining. Badgujar and Rathi [12] detailed the process of optimization by using Taguchi's design and ANOVA analysis in the AWJ machining.

Uthayakumar et al [13] conducted an initial investigation on the ability of AWJ machine to cut

Inconel 600 alloy. Abrasive water-jet milling of aeronautic aluminium 2024-T3 done by Cenac et al [14] with a full experimental design by varying the parameters in multiple levels in order to evaluate the application of AWJ machining for milling of this particular alloy. Aultrin et al [15] used the response surface modelling to AWJ machining of aluminium 6061 alloy and developed a relationship among the parameters and response. Vasanth et al [16] performed the AWJ machining on Ti-6Al-4V alloy using Taguchi's design and identified that abrasive flow rate and standoff distances are the most influential parameters. With the earlier literatures, it was learned that AWJ machining has the potential to machine any material. Identifying the threshold combination of parameters is the most important in AWJ machining. Hence, this paper focuses on studying the effects of various parameters and optimizing the parameters to attain the maximum depth of cut during AWJ machining process on AA 2014.

2. Experimental details

AA 2014 of dimension 100×50×30 mm was chosen as work piece with the chemical composition as shown Table 1. The machining process is performed by vertically mounting the longest side of the work piece to the clamps in the AWJ machine. The study focuses on the traverse speed of the nozzle (S), standoff distance (SOD), pressure of the water jet (P) and mass flow rate (MFR) of abrasive grains. Silicon carbide with 80 meshes is used as the abrasive. The diameter of the orifice and the focusing nozzle used is 0.35/1.1mm. Based on the pilot experiments, the four parameters are varied in three levels to arrive L9 design as per Taguchi's design of experiments as given in Table 2.

Table 1: The chemical composition of AA 2014

Elem.	wt. %	Elem.	wt. %
Cu	4.17	Ti	0.05
Zn	0.15	Mn	0.78
Mg	0.04	Ni	0.06
Si	0.12	Zr	0.07

Table 2: Experimentation design with the depth of cut

S (mm/min)	SOD (mm)	P (MPa)	MFR (kg/min)	Depth of cut (mm)
100	0.5	150	0.25	10.7
100	1.5	250	0.4	23.1
100	2.5	350	0.55	31.5
150	0.5	250	0.55	18.8
150	1.5	350	0.25	18.7
150	2.5	150	0.4	8.3
200	0.5	350	0.4	18.0
200	1.5	150	0.55	9.6
200	2.5	250	0.25	10.8

3. Results and discussion

3.1. Statistical analysis

Using the Taguchi method, the objective function is converted to Signal to Noise (S/N) ratio. The S/N ratio analysis is used in this study to analyse the effect of factors influencing the depth of cut. The depth of cut is taken as the objective function and "Higher the better" quality characteristic of Taguchi's method is chosen to maximize the objective function. The response table for the S/N ratios is shown in Table 3. It is evident that the water pressure is the most influential parameter which affects the depth of cut. The analysis also provides the order in which the factor affects the depth of cut, namely pressure, and traverse speed, mass flow rate of abrasives and standoff distance. The main effect plot obtained from the S/N ratio analysis is shown in Fig. 1. In order to get the maximum depth of cut, the traverse speed must be at its lowest possible level (100 mm/min), the standoff distance must be at its median level (1.5 mm), pressure set to the highest possible level (350 MPa) and mass flow rate be maximum (0.55 kg/min). Furthermore, the main effects plot reveals that pressure has the most influence on the depth of cut followed by traverse speed and mass flow rate.

Table 3: S/N response table for depth of cut

Level	S	SOD	P	MFR
1	25.94	23.73	19.54	22.23
2	23.1	24.12	24.47	23.59
3	21.81	23.01	26.84	25.03
Delta	4.14	1.11	7.3	2.8
Rank	2	4	1	3

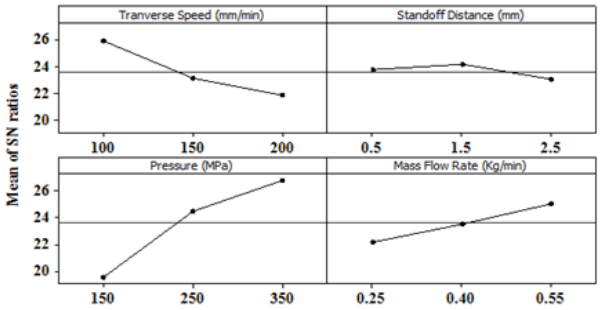

Fig. 1: Main effects plot for depth of cut

The contour band plots indicating regions of the depth of cut are shown in Fig. 2(a-f), where (a) with respect to pressure and traverse speed, (b) with respect to pressure and standoff distance, (c) with respect to mass flow rate and traverse speed, (d) with respect to mass flow rate and standoff distance, (e) with respect to standoff distance and traverse speed, (f) with respect to mass flow rate and pressure. From Fig. 2(a), it is observed that the depth of cut is maximum for lower level of traverse speed (100 mm/min) and highest level of pressure (350 MPa) setting with the values of 30 mm depth and pressure to 150 MPa with traverse speed values increasing upwards of 180mm/min seem to provide the least material removal. From Fig. 2(b), it is observed that the highest level of pressure (350 MPa) and standoff distance (2.5mm) cause the maximum depth of cut and higher level of standoff distance, i.e. above 2.0mm and lower pressure level seems to be the poorest choice of combination for achieving maximum depth of cut as the observed values are less than 10mm in depth. In Fig. 2(c), it is observed that the maximum depth of cut is observed when the mass flow rate is above 0.5kg/min with the traverse speed set to around 100mm/min and lower depth of cut at medium levels of mass flow rate and traverse speed.

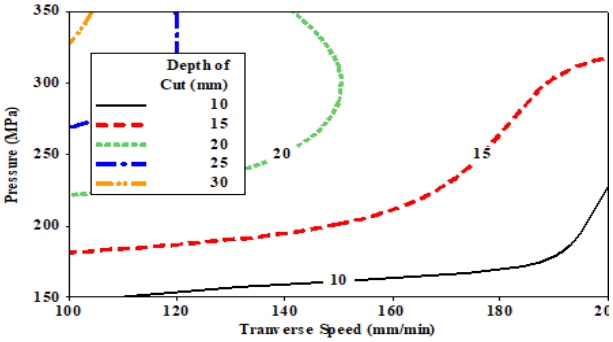

Fig. 2(a): Contour plots for depth of cut concerning pressure, traverse speed

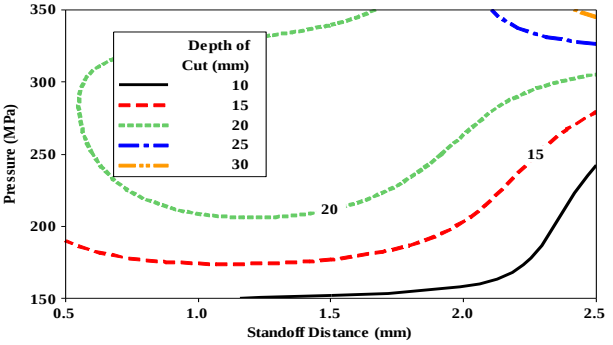

Fig. 2(b): Contour plots for depth of cut concerning pressure, standoff distances

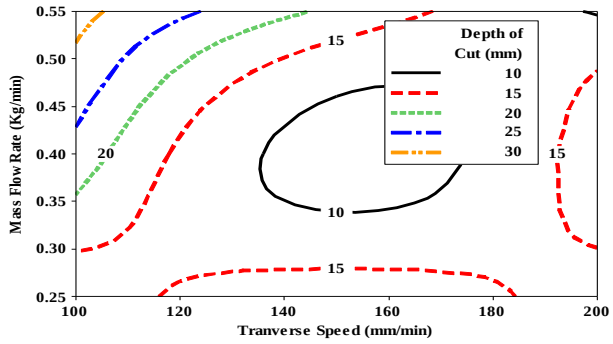

Fig. 2(c): Contour plots for depth of cut concerning mass flow rate, traverse speed

From Fig. 2(d), it is observed that the depth of cut is the maximum for higher level of mass flow rate (above 0.50 kg/min) and highest level of standoff distance (2.5mm) and the mass flow rate below 0.40 kg/min with standoff distance values increasing upwards of 2.5 mm seem to provide the least material removal and less than 10mm depth of cut observed. Fig. 2(e) shows the contour plot between standoff distance and the traverse speed. It is seen that the maximum depth of cut (upwards of 30 mm) forms when the standoff distance is set to its highest-level setting of 2.5 mm and traverse speed is kept low at 100 mm/min. The plot seems diverge from this region outwards, i.e. with increasing traverse speed, the depth of cut is seen to be lowered. The minimum depth of cut region is formed when the standoff distance is kept between 1.5-2.5 mm and traverse speed values increase upwards of 150 mm/min. Fig. 2(f) appears to be a vertically mirrored image of Fig. 2(e), i.e. the highest levels of mass flow rate and pressure seem to create the maximum depth of cut. With decreasing level of both parameters, the depth of cut is observed to reduce. The lowest depth of cut region forms when the pressure is at its lowest setting of 150 MPa, immaterial of any setting of mass flow rate chosen. The depth of cut is above 30mm when the mass flow rate is set to 0.55kg/min and pressure set to its highest level of 350MPa.

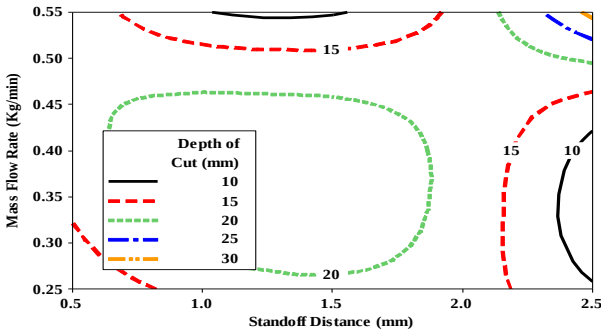

Fig. 2(d): Contour plots for depth of cut concerning mass flow rate, standoff distance

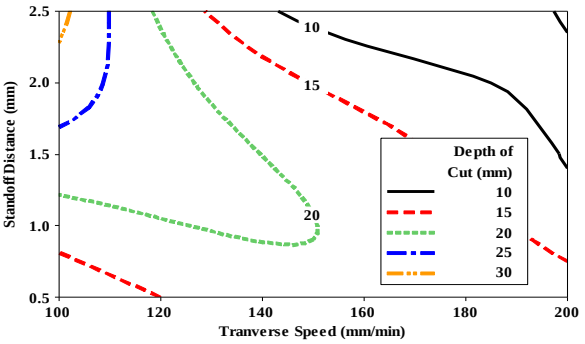

Fig. 2(e): Contour plots for depth of cut concerning standoff distance, traverse speed

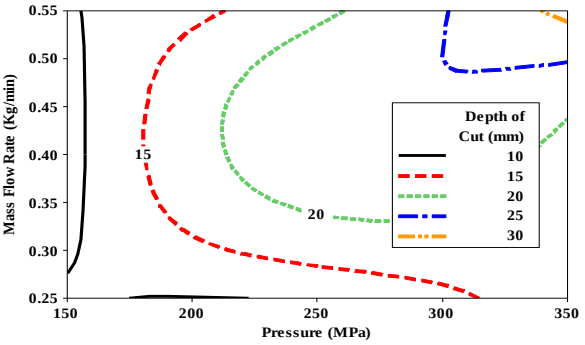

Fig. 2(f): Contour plots for depth of cut concerning mass flow rate, pressure

3.2. Analysis of variance

The ANOVA analysis is used in this study to find out the significance of each factor as shown in Table 4 with a computed R-square value of 99.39%.

Table 4: Analysis of variance for depth of cut

Source	DF[a]	Seq SS[b]	Adj SS[c]	Adj MS[d]	F	P[e]
S (mm/min)	2	128.73	128.73	64.36	45.51	0.02
P (MPa)	2	265.46	265.46	132.73	93.84	0.011
MFR(kg/min)	2	64.776	64.77	32.38	22.9	0.042
Error	2	2.829	2.82	1.41	-	-
Total	8	461.80	-	-	-	-

[a]Degrees of freedom, [b]Sequential sums of squares, [c]Adjusted sums of squares, [d]Adjusted mean squares, [e]Probability.

It is identified that the most significant parameters in depth of cut are pressure of water jet followed by the traverse speed, with the contribution of 93.84% and

45.51% respectively. The effects of mass flow rate on the depth of cut is, however, lower than estimated and is meagre in comparison to other factors.

3.3. Regression analysis

A first order linear regression equation is formulated to predict the depth of cut value within specified level values of significant parameters with the regression coefficient value of 97.06% is given as,

$$Depth\ of\ cut\ = 4.03056 - 0.0896667 * S + 0.51666 * SOD + 0.066 * P + 21.8889 * MFR$$

Fig. 3 represents the normal probability plot for depth of cut. It is evident that the residuals (errors) are normally distributed along a straight line.

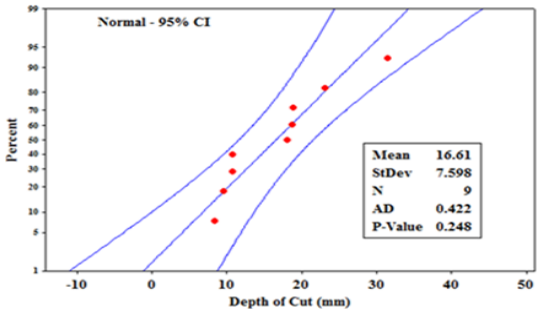

Fig. 3: Normal probability plot for depth of cut

3.4. Confirmation test

In order to validate the results, a confirmation test as shown in Table 5 was conducted based on the optimum combination level of A1B2C3D3. It is observed that the predicted value and observed value are deviated only by a small error percentage of 0.30%.

Table 5: Confirmation test for depth of cut

Level	Predicted A1B2C3D3	Experimental A1B2C3D3	Error
Depth of cut (mm)	31.7667	31.67	0.30%

4. Conclusion

AWJ machining on aluminium alloy 2014 with Taguchi's L9 array design was performed and following are the conclusions are made:

- From the S/N ratio analysis response table and the main effects plot, it was identified that the pressure of water jet was the most influential factor in creating a large depth of cut followed by traverse speed.
- The optimal level combination of parameters that cause the largest depth of cut was identified as A1B2C3D3, i.e. traverse speed of 100mm/min, a standoff distance of 1.5mm, the pressure of 350MPa and a mass flow rate of 0.55 kg/min.
- The ANOVA revealed that the significant parameters with respect to the depth of cut are pressure and traverse speed with F contribution of 93.84% and 45.51% respectively.
- A linear regression equation was formulated to predict the depth of cut values for a given set of parameter combination.
- Finally, a confirmation test was conducted, and the tests showed a meagre error value of 0.30%.

REFERENCES:

[1] H. Hocheng and K.R. Chang. 1994. Material removal analysis in abrasive water jet cutting of ceramic plates, *J. Materials Proc. Tech.*, 40(3-4), 287-304. https://doi.org/10.1016/0924-0136(94)90456-1.

[2] G.S. Choi and G.H. Choi. 1997. Process analysis and monitoring in abrasive water jet machining of alumina ceramics, *Int. J. Machine Tools and Manu.*, 37(3), 295-307. https://doi.org/10.1016/S0890-6955(96)00049-1.

[3] A.W. Momber and R. Kovacevic. 1997. Test parameter analysis in abrasive water jet cutting of rocklike materials. *Int. J. Rock Mechanics and Mining Sci.*, 34(1), 17-25. https://doi.org/10.1016/S1365-1609(97)80030-5.

[4] H. Hocheng, H.Y. Tsai, J.J. Shiue and B. Wang. 1997. Feasibility study of abrasive-water jet milling of fibre-reinforced plastics, *J. Manuf. Sci. and E*ngg., 119(2), 133-142. https://doi.org/10.1115/1.2831088.

[5] J. Wang and W.C. Wong. 1999. A study of abrasive water jet cutting of metallic coated sheet steels, *Int. J. Machine Tools and Manuf.*, 39(6), 855-870. https://doi.org/10.1016/S0890-6955(98)00078-9.

[6] C.Z. Huang, R.G. Hou, J. Wang and Y.X. Feng. 2006. The effect of high pressure abrasive water jet cutting parameters on cutting performance of granite, *Key Engg. Materials*, 304, 560-564. https://doi.org/10.4028/0-87849-986-5.560.

[7] M.A. Azmir, A.K. Ahsan and A. Rahmah. 2009. Effect of abrasive water jet machining parameters on aramid fibre reinforced plastics composite, *Int. J. Material Forming*, 2(1), 37-44. https://doi.org/10.1007/s12289-008-0388-2.

[8] D.A. Axinte, D.S. Srinivasu, M.C. Kong and P.W.B. Smith. 2009. Abrasive water jet cutting of polycrystalline diamond: A preliminary investigation, *Int. J. Machine Tools and Manufacture*, 49(10), 797-803. https://doi.org/10.1016/j.ijmachtools.2009.04.003.

[9] J. Kechagias, G. Petropoulos and N. Vaxevanidis. 2012. Application of Taguchi design for quality characterization of abrasive water jet machining of trip sheet steels, *Int. J. Advanced Manuf. Tech.*, 62(5-8), 635-643. https://doi.org/10.1007/s00170-011-3815-3.

[10] V. Gupta, P.M. Pandey, M.P. Garg, R. Khanna and N.K. Batra. 2014. Minimization of kerf taper angle and kerf width using Taguchi's method in abrasive water jet machining of marble, *Proc. Materials Sci.*, 6, 140-149. https://doi.org/10.1016/j.mspro.2014.07.017.

[11] F. Kartal, M.H. Çetin, H. Gökkaya and Z. Yerlikaya. 2014. Optimization of abrasive water jet turning parameters for machining of low density polyethylene material based on experimental design method, *Int. Polymer Proc.*, 29(4), 535-544. https://doi.org/10.3139/217.2925.

[12] P.P. Badgujar and M.G. Rathi. 2014. Taguchi method implementation in abrasive water jet machining process optimization, *Int. J. Engg., and Advanced Tech.*, 3(5), 66-70.

[13] M. Uthaya kumar, M.A. Khan, S.T. Kumaran, A. Slota and J. Zajac. 2016. Machinability of nickel-based superalloy by abrasive water jet machining, *Materials and Manuf. Proc.*, 31(13), 1733-1739. https://doi.org/10.1080/10426914.2015.1103859.

[14] F. Cenac, R. Zitoune, F. Collombet and M. Deleris. 2015. Abrasive water-jet milling of aeronautic aluminum 2024-

T3, *Proc. IMechE Part L: J. Materials: Design and Applications*, 229(1), 29-37.

[15] K.J. Aultrin and M.D. Anand. 2014. Experimental framework and study of AWJM process for an aluminium 6061 alloy using RSM, *Control, Instrumentation, Communication and Computational Techn.*, 1432-1440.

[16] S. Vasanth, T. Muthuramalingam, P. Vinoth kumar, T. Geethapriyan and G. Murali. 2016. Performance analysis of process parameters on machining titanium (Ti-6Al-4V) alloy using abrasive water jet machining process, *Proc. CIRP*, 46, 139-142. https://doi.org/10.1016/j.procir.2016.04.072.